

A new highly precise weak gravitational lensing flexions measurement method based on ERA method.

Yuki Okura,^{1,2}★ Toshifumi Futamase,³

¹*NAOJ*

²*RIKEN*

³*Kyoto Sangyo University*

11 June 2022

ABSTRACT

Weak gravitational lensing flexions are a kind of weak lensing distortion which are defined as the spin 1 and spin 3 combinations of the third order derivatives of gravitational lensing potential. Since the shear has spin 2 combination of the second order derivative, the flexion signal gives a partly independent information from shear signal and is more sensitive to the local mass distribution than shear signal. Thus its measurement is expected to play important roles in observational cosmology. However, since the weakness of the flexion signal as well as the complicatedness of its intrinsic noise made its accurate observation very difficult. We propose a new method of measuring the flexion signal using ERA method which is a method to measure weak lensing shear without any approximation. We find two particular combinations of the flexions which provide the quantities with only lensing information and free of intrinsic noise when taken average. It is confirmed by simple numerical simulation that the statistical average of these combinations do not in fact depend on the strength of the intrinsic distortion.

arXiv:2109.00155v1 [astro-ph.CO] 1 Sep 2021

1 INTRODUCTION

It is widely recognized that weak gravitational lensing shear analysis is a unique and powerful tool to analyze the mass distribution of the universe. Coherent deformation of the shapes of background galaxies carries not only the information of intervening mass distribution but also the cosmological background geometry and thus the cosmological parameters (Mellier 1999; Schneider 2006; Munshi et al. 2008).

Weak gravitational flexions are defined from the third derivative of gravitational lensing potential (Goldberg and Natarajan 2002, Goldberg and Bacon 2005, Bacon, et al., 2006), hence it is more sensitive to small scale mass structure than shear which is defined as the second derivative of lensing potential. This fact means that the flexion measurement will be very useful to measure small scale mass structure, e.g. sub-halos of galaxy clusters.

Measurement of small scale mass variation is also very important for studying mass evolution in non-linear scale by statistical weak lensing analysis such as cosmic flexion or galaxy-galaxy flexion. The science will be done by current and future wide field survey such as Hyper Suprime-Cam¹ (HSC), Kilo-Degree Survey² (KiDS), The Deep Lens Survey³ (DLS), Canada-France-Hawaii Telescope Legacy Survey⁴ (CFHTLS) Dark Energy Survey⁵ (DES), and are planned such as The Large Synoptic Survey Telescope⁶ (LSST), EUCLID⁷ (EUCLID), Wide Field Infrared Survey Telescope⁸ (WFIRST). As an example, the Hyper Suprime-Cam Subaru Strategic Program (SSP) is planning 1400 deg² wide survey observation for constraining the cosmological parameters with less than 1% uncertainty. The observation started in 2014, and 100 deg² of HSC wide survey data was recently published. To achieve a severe constraint on the equation of state parameter for dark energy, the HSC SSP requires a highly precise weak gravitational lensing shear analysis method with lower than 1% systematic error.

The flexion measurement using such a huge and detailed data is highly expected to withdraw important sciences hidden in the data. However the actual analysis of flexion measurement is very difficult because of the smallness of the flexion signal as well as complicated intrinsic noise. Some methods to measure the flexion have been developed (Irwin and Shmakova 2006, Irwin et al. 2007, Goldberg and Leonard 2007, Levinson 2013) and mass distribution of some regions were reconstructed from measured flexion (Leonard et al. 2009, Bird and Goldberg 2018), then the application of flexion to small scale mass distribution has studied (Bacon et al. 2010). And recently, the improvement of mass reconstruction using flexion and intrinsic flexion information has been studied (Benjamin Cain 2016, Cardone 2016, Lanusse 2016, Joseph 2020).

We already developed a method to measure flexions (Okura, Umetsu and Futamase, 2007) with PSF correction, and applied the method to reconstruct the mass distribution of the Abell 1689 galaxy cluster and revealed two peak structures in the central region. However, our analysis considered only the spin 1 part of flexion and did not consider the combination of flexion and shear (ellipticity). Furthermore the noise analysis associated with the flexion measurement was insufficient. Thus it is desirable to develop more precise flexion measurement analysis for precise mass reconstructions and sciences.

In this paper we formulate an accurate flexion measurement method based on the technique we have developed to improve the accuracy of shear measurement (Okura and Futamase 2011, 2012, 2013, 2014, 2015, 2016 and 2018). In particular, the ERA method of PSF (Point Spread Function) correction plays a central role in our method. In the ERA method, PSF correction is done by re-smearing the PSF and the observed galaxy image using the re-smearing function. In this way we can use a new PSF with a simple shape and correct the PSF effect. The method does not use any approximation to measure shear, so it does not have the systematic error in PSF correction. The details of the ERA method can be seen in Okura 2018.

In section 2, we explain the basics about weak lensing and the basics of ERA method for shear measurement. In section 3, we explain the basics of flexions. In section 4, we explain the method to measure flexions. In section 5, we summarize our conclusion.

2 WEAK LENSING AND ERA METHOD

In this section, we explain the basics about weak lensing and the basics about ERA method for shear measurement. In this paper, we use complex for two-dimensional value, e.g. two dimensional coordinates, and it is notated by bold font.

2.1 Lensing distortion

Gravitational lensing effect deflects the path of light ray from the source object by the lensing object such as star, galaxy and a cluster of galaxies. Let the angular position of the object on the celestial sphere be β without lensing and θ with lensing effect. The two-position is related by a derivative of gravitational lensing potential Φ , as follows.

$$\beta = \theta - \partial\Phi(\theta), \quad (1)$$

then the coordinate β is called “source plane” and the coordinate θ is called “image plane”.

¹ <http://www.naoj.org/Projects/HSC/HSCProject.html>

² <http://kids.strw.leidenuniv.nl/>

³ <http://matilda.physics.ucdavis.edu/working/website/index.html>

⁴ <http://www.cfht.hawaii.edu/Science/CFHTLS/>

⁵ <https://www.darkenergysurvey.org/>

⁶ <http://www.lsst.org>

⁷ <http://sci.esa.int/euclid>

⁸ <https://wfirst.gsfc.nasa.gov/>

Let $d\beta = \beta - \bar{\beta}$ and $d\theta = \theta - \bar{\theta}$ be infinitesimal angular deviation from the centroid of the object image in the source plane $\bar{\beta}$ and in the image plane $\bar{\theta}$, respectively. If the object is at the position that the lensing effect is weak, the relation between the lengths can be described as

$$d\beta = (1 - \kappa) d\theta - \gamma_L d\theta^* \equiv (1 - \kappa) (d\theta - g_L d\theta^*), \quad (2)$$

where κ and γ_L are weak gravitational lensing convergence and shear defined as 2nd deviation of the lensing potential

$$\kappa \equiv \frac{1}{2} \partial \partial^* \Phi \quad (3)$$

$$\gamma_L \equiv \frac{1}{2} \partial \partial \Phi, \quad (4)$$

and g_L is reduced shear defined as $g_L \equiv \gamma_L / (1 - \kappa)$. The equation 2 means convergence changes the size and shear changes ellipticity of the object between source plane and image plane.

2.2 Zero plane

The ERA method uses the idea of “zero planes”. The zero plane is an artificial plane with the coordinate $\tilde{\beta}$ where the object has a circular shape “zero image”, so the zero image has zero ellipticity, then the intrinsic shape can be expressed as the distortion from the zero plane.

Let g_I and g_L be intrinsic and lensing reduced shear respectively, then the relation between the zero and the source plane is described as

$$d\tilde{\beta} = d\beta - g_I d\beta^*. \quad (5)$$

By using equation 1, the relation between zero plane and image plane is described as

$$\begin{aligned} d\tilde{\beta} &= d\beta - g_I d\beta^* = (1 + g_I g_L^*) d\theta - (g_I + g_L) d\theta^* \\ &\equiv (1 + g_I g_L^*) (d\theta - g_C d\theta^*) \end{aligned} \quad (6)$$

$$g_C \equiv \frac{g_I + g_L}{1 + g_I g_L^*}, \quad (7)$$

where $(1 + g_I g_L^*)$ is just a size change and rotation, so it can be ignored in zero plane, and g_C is combined with reduced shear and it is the same as the ellipticity of the object in the image plane. Finally, by the ignoring, the lensing equation between zero plane and image plane can be described as

$$d\tilde{\beta} = d\theta - g_C d\theta^*. \quad (8)$$

The lensing shear g_L can be obtained by a simple average of the combined shear g_C . Let’s describe the intrinsic shear distribution in polar coordinate as

$$g_I = g(r) e^{i\phi}, \quad (9)$$

where $g(r)$ is unknown radial distribution of the intrinsic shear with normalization

$$\int_0^{2\pi} d\phi \int_0^1 r dr g(r) = 2\pi \int_0^1 r dr g(r) = 1. \quad (10)$$

The simple average of the combined shear with infinite number of background galaxies can be described as

$$\begin{aligned} \langle g_C \rangle &= \int_0^{2\pi} d\phi \int_0^1 r dr \frac{g_I + g_L}{1 + g_I g_L^*} \\ &= \int_0^1 r dr \int_0^{2\pi} d\phi \frac{g(r) e^{i\phi} + g_L}{1 + g(r) e^{i\phi} g_L^*} \\ &= 0 + g_L \int_0^1 r dr 2\pi g(r) = g_L. \end{aligned} \quad (11)$$

The notations used here after this paper are listed in table 1.

2.3 Zero moments and shapes

ERA method defines complex image moments \mathcal{M}_M^N of object image $A(\theta) = \tilde{A}(\tilde{\beta})$ in “zero plane” as

$$\mathcal{M}_M^N \equiv \int d^2 \tilde{\beta} d\tilde{\beta}_N^M \tilde{A}(\tilde{\beta}) \tilde{W}(|d\tilde{\beta}|) = \int d^2 \theta J(\theta) \left(d\tilde{\beta}(\theta) \right)_N^M A(\theta) W(d\theta) \quad (12)$$

$$d\tilde{\beta}_N^M = d\tilde{\beta}^{\frac{M+N}{2}} d\tilde{\beta}^{*\frac{M-N}{2}} \quad (13)$$

$$J(\theta) \equiv \left| \frac{d^2 \tilde{\beta}}{d^2 \theta} \right|, \quad (14)$$

| notation | definition |
|--------------------|--|
| $\tilde{\beta}$ | Coordinate in zero plane, the basis is the centroid of the object. |
| β | Coordinate in source plane, the basis is centroid of object. |
| θ | Coordinate in image plane, the basis is centroid of object. |
| \mathbf{g} | Weak gravitational lensing reduced shear. |
| \mathcal{F} | Weak gravitational lensing reduced first flexion. |
| \mathcal{G} | Weak gravitational lensing reduced second flexion. |
| \mathcal{H} | Weak gravitational lensing reduced third flexion. |
| \mathcal{F}_L | Lensing first flexion. |
| \mathcal{F}_I | Intrinsic first flexion. |
| \mathcal{F}_C | Combined first flexion. |
| \mathcal{F}_E | Eigen first flexion. |
| $\mathcal{F}_{E'}$ | Eigen first flexion combination. |
| A | Arbitrary object image. |
| W | Weight function. |
| M | Mask function. |
| J | Jacobian. |
| \mathcal{M}_M^N | zero moment. N is order and M is spin-number. |

Table 1. Notations used after next sections. These notations about image and functions are in the case of image plane, these functions in zero plane are notated with tilde, i.e. A is in image plane and \tilde{A} is in zero plane, then these functions in Fourier space is notated with hat, i.e. \hat{A} in Fourier space. The subscription of \mathcal{F}_L , \mathcal{F}_I , \mathcal{F}_C , \mathcal{F}_E and $\mathcal{F}_{E'}$ are used for shear second flexion and third flexion with same meaning.

where $\tilde{W}(|d\tilde{\beta}|)$ is a weight function for reducing noise from random count and $J(\theta)$ is Jacobian. Since the object image is circular in the zero plane, the image moment with non-zero spin number must have 0 value, so the moment is called “Zero moment”.

The shapes of the object image, centroid and ellipticity, can be measured by finding the centroid of object $\bar{\theta}$ and combined reduced shear \mathbf{g} which makes some zero moments zero, so

$$\mathcal{M}_1^1 = \int d^2\tilde{\beta} d\tilde{\beta}_1^1 \tilde{A}(\tilde{\beta}) \tilde{W}(|d\tilde{\beta}|) = \frac{1}{1 - |\mathbf{g}_C|^2} \int d^2\theta (d\theta - \mathbf{g}_C d\theta^*) A(\theta) W(d\theta) = 0 \quad (15)$$

$$\mathcal{M}_2^2 = \int d^2\tilde{\beta} d\tilde{\beta}_2^2 \tilde{A}(\tilde{\beta}) \tilde{W}(|d\tilde{\beta}|) = \frac{1}{1 - |\mathbf{g}_C|^2} \int d^2\theta (d\theta - \mathbf{g}_C d\theta^*)^2 A(\theta) W(d\theta) = 0, \quad (16)$$

where $\tilde{W}(|d\tilde{\beta}|) = W(d\theta)$ is a weight function for reducing error in shape measurement from pixel noise on and around the galaxy image, and it must be a circular function in zero plane.

In real analysis, we should use an additional mask for weight function in the reversed region. We explain about this mask in the appendix A.

3 WEAK GRAVITATIONAL FLEXIONS

In this section, we explain the basics of weak gravitational flexions.

3.1 The basics of weak gravitational flexions

In the limit of weak lensing, lensing effects change only the ellipticity of the image of the background object. However, in the neighborhood of the strong lensing region, the lensing effect makes images of background galaxies an arc shape. Since the reduced shear, second-order deviation of lensing potential can take into account only change of ellipticity, information of the higher-order deviation of the lensing potential must be needed to take into account arc shape.

The higher-order lensing effect for infinitesimal length is obtained by expanding lensing equation 1 until the third deviation of lens potential, so the lensing equation with flexion is described as

$$\begin{aligned} d\beta &= (1 - \kappa) d\theta - \gamma_L d\theta^* - \frac{1}{4} \left(2F_L d\theta_0^2 + F_L^* d\theta_2^2 + G_L d\theta_{-2}^2 \right) \\ &\equiv (1 - \kappa) \left(d\theta - \mathbf{g}_L d\theta^* - \frac{1}{4} \left(2\mathcal{F}_L d\theta_0^2 + \mathcal{F}_L^* d\theta_2^2 + \mathcal{G}_L d\theta_{-2}^2 \right) \right), \end{aligned} \quad (17)$$

where F_L and G_L are first flexion and second flexion respectively, these are defined as the third deviation of lensing potential as

$$F_L \equiv \partial\partial\partial^*\Phi \quad (18)$$

$$G_L \equiv \partial\partial\partial\Phi. \quad (19)$$

and $\mathcal{F}_L = F_L/(1 - \kappa)$ and $\mathcal{G}_L = G_L/(1 - \kappa)$ are first and second reduced flexion.

3.2 Intrinsic Flexion and Combined Flexions

In this section, we define the combined flexions by intrinsic flexions, namely, the first flexion and second flexion. The definition will be made in the same way as section 2.2.

Let the distortions (shear, first flexion and second flexion) with subscript I mean intrinsic distortion, then the relations between the zero plane and the source plane is described as

$$d\tilde{\beta} = d\beta - g_I d\beta^* - \frac{1}{4} \left(2\mathcal{F}_I d\beta_0^2 + \mathcal{F}_I^* d\beta_2^2 + \mathcal{G}_I d\beta_{-2}^2 \right). \quad (20)$$

Using equation 17 and , the relation between the image plane and the zero plane with flexion are described as

$$d\tilde{\beta} = (1 - \kappa) (1 + g_I g_L^*) \left(d\theta - g_C d\theta^* - \frac{1}{4} \left(2\mathcal{F}_C d\theta_0^2 + \mathcal{H}_C d\theta_2^2 + \mathcal{G}_C d\theta_{-2}^2 \right) \right) \quad (21)$$

where the combined flexions $\mathcal{F}_C, \mathcal{G}_C, \mathcal{H}_C$ are defined as follows

$$\mathcal{F}_C \equiv \frac{\mathcal{F}_L + \mathcal{F}_I - g_I \mathcal{F}_L^* + |g_L|^2 \mathcal{F}_I - g_L \mathcal{F}_I^* - g_L^* \mathcal{G}_I}{1 + g_I g_L^*} \quad (22)$$

$$\mathcal{G}_C \equiv \frac{\mathcal{G}_L + \mathcal{G}_I - g_I \mathcal{F}_L - 2g_L \mathcal{F}_I + g_L^2 \mathcal{F}_I^*}{1 + g_I g_L^*} \quad (23)$$

$$\mathcal{H}_C \equiv \frac{\mathcal{F}_L^* + \mathcal{F}_I^* - g_I \mathcal{G}_L^* - 2g_L^* \mathcal{F}_I + g_L^{*2} \mathcal{G}_I}{1 + g_I g_L^*}, \quad (24)$$

where we call \mathcal{H}_C as the third flexion in this paper, and here after $(1 - \kappa) (1 + g_I g_L^*)$ is ignored for the same reason explained in section 2.2.

The above equations mean, that the conjugate of \mathcal{H}_C has spin 1 and is similar as \mathcal{F}_C , but the differences from \mathcal{F}_C contain variables such as g_L (lensing distortion) and g_I (intrinsic distortion) which are not obtained from the measurement of the individual images. Thus these 3 quantities are independent. On the other hand the moments we measure are only \mathcal{M}_1^3 and \mathcal{M}_3^3 . This causes a serious problem in the flexion measurement. To determine three flexions uniquely, a constraint condition is needed, however it is conceivable that the general condition may depend on the intrinsic and the lensing distortions which cannot be obtained in shape measurement of each object. We need to find a particular condition in such a way that the resultant flexions do not produce any systematic error.

We calculate the value of the ensemble average of the three combined flexions using a simple simulated image and two constraint conditions. In this simulation we used a simple Gaussian image which has 4 pixels Gaussian radius. We make a lensed image by applying intrinsic and lensing distortions to the Gaussian image. We used two standard deviation sets as intrinsic distortions. One is weak noise (WN) with $\sigma_g = 0.2$, $\sigma_{\mathcal{F}} = 0.001$ and $\sigma_{\mathcal{G}} = 0.001$, and another one is strong noise (SN) with $\sigma_g = 0.3$, $\sigma_{\mathcal{F}} = 0.005$ and $\sigma_{\mathcal{G}} = 0.005$. Then we used two lensing distortions. One is weak arc (WA) with $g_L = -0.3$, $\mathcal{F}_L = -0.005$ and $\mathcal{G}_L = 0.005$, and another one is a strong arc (SA) with $g_L = -0.6$, $\mathcal{F}_L = -0.01$ and $\mathcal{G}_L = 0.01$. Figure 1 shows sample images which are Gaussian images distorted by only the lensing distortions.

A conjugate of the third flexion \mathcal{H}_C is equal to \mathcal{F}_C up to the first order, so the first one of the constraint condition we use in this simulation is

$$\mathcal{H}_C = \alpha \mathcal{F}_C^* \quad (25)$$

with variable α . Figure 2 to 7 show the ensemble average of the combined flexions for variable α of the constraint condition. Then, the second one of the constraint condition is simply applying constant for \mathcal{H}_C , so

$$\mathcal{H}_C = \beta \quad (26)$$

Figure 8 to 10 show the ensemble average with variable β of the constraint condition only for the data set (SN, SA). We can see the combined flexions strongly depend on not only strength of intrinsic noise but also selection of the constraint condition.

4 A NEW METHOD FOR FLEXION PRECISE MEASUREMENT WITH REMOVING INTRINSIC NOISE

4.1 eigen flexion values and lensing information

In the previous section, it was shown that systematic error occurs because of the wrong choice of the constraint condition, or the wrong choice of the quantities we measure. In fact it turns out that the latter is the case and we can find two kinds of combination of the combined flexions whose average is independent of the selection of the constraint condition. We call these combinations as eigen flexions.

In deriving the eigen flexions, we use the ERA method where the zero image in the zero plane has circular shape with arbitrary radial profile. This means that the brightness distribution of zero image is a function with variable $|d\tilde{\beta}|^2$. Then the variable is transformed in the lens plane up to the first-order in flexion as

$$|d\tilde{\beta}|^2 = (1 - \kappa)^2 |1 + g_I g_L^*|^2 \left((1 + |g_C|^2) d\theta_0^2 - 2\text{Re} [g_C^* d\theta_2^2] - \frac{1}{2} \left(\text{Re} [\mathcal{F}_E^* d\theta_1^3] + \text{Re} [\mathcal{G}_E^* d\theta_3^3] \right) \right) \quad (27)$$

$$\mathcal{F}_E \equiv 2\mathcal{F}_C + \mathcal{H}_C - 2g_C \mathcal{F}_C^* - g_C^* \mathcal{G}_C \quad (28)$$

$$\mathcal{G}_E \equiv \mathcal{G}_C - g_C \mathcal{H}_C^* \quad (29)$$

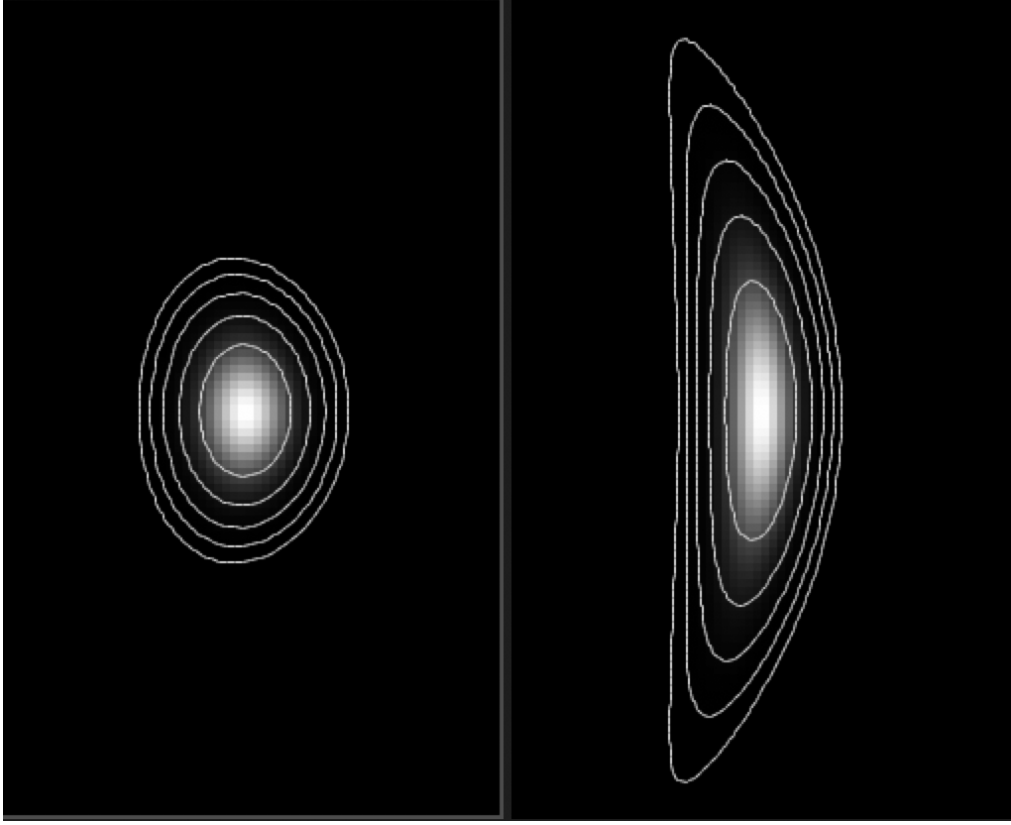


Figure 1. Gaussian images with the lensing distortion which is used in the simulation test in this paper. The left side image, weak arc(WA), is distorted by lensing distortion $\mathbf{g} = -0.3$, $\mathcal{F} = -0.005$ and $\mathcal{G} = 0.005$, and the right image, strong arc(SA), is distorted by lensing distortion $\mathbf{g} = -0.6$, $\mathcal{F} = -0.01$ and $\mathcal{G} = 0.01$. The brightness of the image is linear scale, but the contour is log scale for visibility of arc shape.

Natural combinations of the combined flexions appear here. This equation means that the brightness distribution of the lensed image is a function with variables \mathbf{g}_C , \mathcal{F}_E and \mathcal{G}_E , and the flexion effect is described by \mathcal{F}_E and \mathcal{G}_E . We call these as eigen flexions.

Using the simulation described in the previous section, we have confirmed the independence of the eigen flexion from the choice of the above two constraint conditions with the same simulation test as the previous section. (Actually we have checked the independence of the result using other constraint conditions.) Figures 11 to 16 are the result of the simulation test. We can see the fluctuations of the average of the eigen flexion decrease compared to the average of the combined flexions. So, we can obtain the eigen flexion \mathcal{F}_E and \mathcal{G}_E by using arbitrary convenient value of the parameter in the constraint condition from the combined flexion \mathcal{F}_C and \mathcal{G}_C . However the eigen flexions are useless in their present forms because they contain the intrinsic shear term $|\mathbf{g}_I|^2$ which does not vanish after averaging. This means that the ensemble average of the eigen flexions have systematic error due to intrinsic noise.

We have found a combination of eigen flexion which do not include $|\mathbf{g}_I|^2$ as follows

$$\mathcal{F}_{E'} \equiv \frac{\mathcal{F}_E + \mathbf{g}_C^* \mathcal{G}_E + \mathbf{g}_C \mathcal{F}_E^* + \mathbf{g}_C^2 \mathcal{G}_E^*}{1 - |\mathbf{g}_C|^2} = 2\mathcal{F}_C + \mathcal{H}_C^* + \mathbf{g}_C \mathcal{H}_C \quad (30)$$

$$\mathcal{G}_{E'} \equiv \frac{\mathcal{G}_E + \mathbf{g}_C \mathcal{F}_E + \mathbf{g}_C^2 \mathcal{F}_E^* + \mathbf{g}_C^3 \mathcal{G}_E^*}{1 - |\mathbf{g}_C|^2} = \mathcal{G}_C + 2\mathbf{g}_C \mathcal{F}_C + \mathbf{g}_C^2 \mathcal{H}_C. \quad (31)$$

Finally, by taking ensemble average of them, we can remove intrinsic distortions,

$$\langle \mathcal{F}_{E'} \rangle = 3\mathcal{F}_L + \mathbf{g}_L \mathcal{F}_L^* \quad (32)$$

$$\langle \mathcal{G}_{E'} \rangle = \mathcal{G}_L + 2\mathbf{g}_L \mathcal{F}_L + \mathbf{g}_L^2 \mathcal{F}_L^*, \quad (33)$$

where we assume that the intrinsic distortions are independent of each other. Equation 32 and 33 still contain lensing shear \mathbf{g}_L , but it can be obtained by ensemble average of combined shear \mathbf{g}_C . We call the two flexions $\langle \mathcal{F}_{E'} \rangle$ and $\langle \mathcal{G}_{E'} \rangle$ as an eigen (first and second) flexion combination.

We investigate the eigen flexion combinations by the same simulation in the combined flexions. Figures 17 to 22 are plots of the ensemble average of the eigen flexion combinations measured from the simulated images. We can see the average value does not depend on the strength of intrinsic distortions, so the their average values have only the lensing information and coincide correctly with the given values.

It is confirmed that the ensemble average of the eigen flexion combinations have only lensing information, so finally, after obtaining \mathbf{g}_L

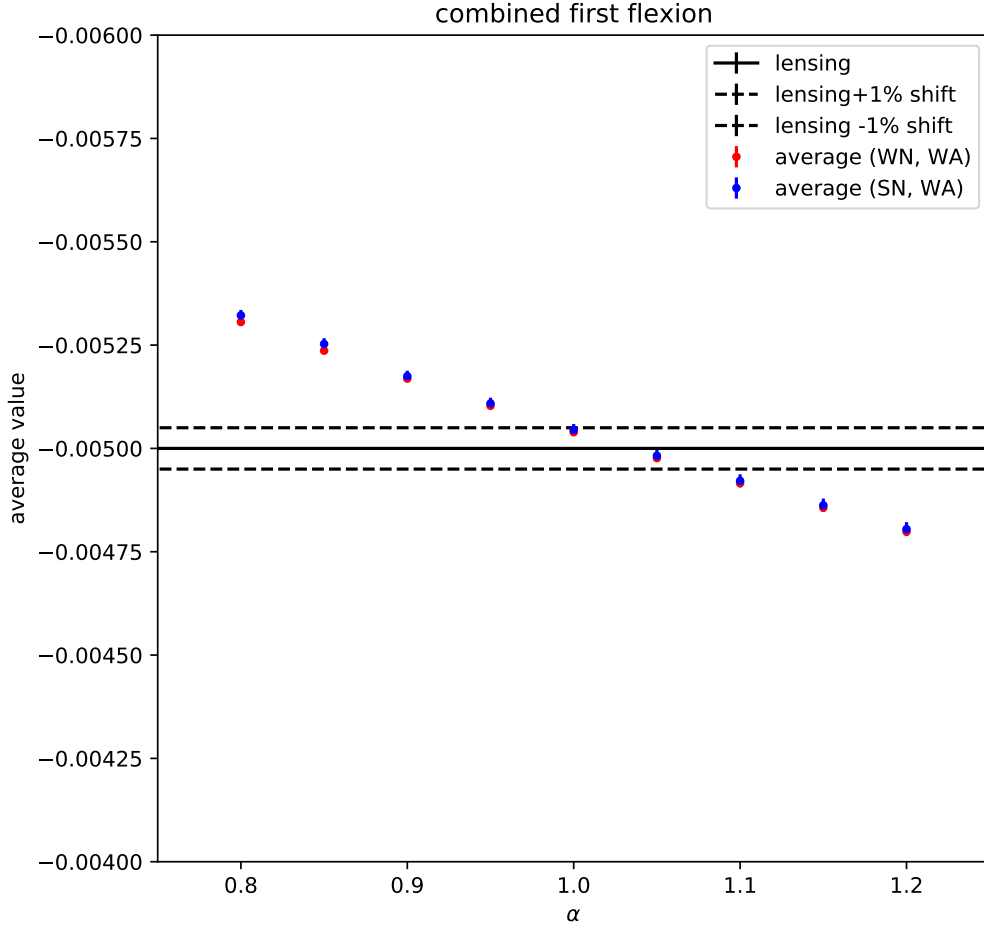


Figure 2. The average value of the combined first flexion as a function of the constraint condition Cc. The red and blue points are in the case of (WN, WA) and (SN, WA) respectively. The solid line is combined first flexion without any intrinsic distortions, so lensing first flexion. We can see the average values are strongly depended on the constraint condition, and the average values are different from lensing value in most of Cc range.

from $\langle g_C \rangle$, we can obtain weak gravitational lensing flexions as

$$\mathcal{F}_L = \frac{3 \langle \mathcal{F}_{E'} \rangle - \langle g_C \rangle \langle \mathcal{F}_{E'} \rangle^*}{9 - |\langle g_C \rangle|^2} \quad (34)$$

$$\mathcal{G}_L = \langle \mathcal{G}_{E'} \rangle - \langle g_C \rangle \frac{(6 - |\langle g_C \rangle|^2) \langle \mathcal{F}_{E'} \rangle + \langle g_C \rangle \langle \mathcal{F}_{E'} \rangle^*}{9 - |\langle g_C \rangle|^2}, \quad (35)$$

5 SUMMARY

In this paper, we developed a new precise flexions measurement method. Flexions appeared in third order terms in the expansion of the lensing equation than shear, so the formulas to measure flexions are much more complicated than that of shear.

We applied the idea of the zero plane to calculate the relation between the image plane and the zero plane. In the course of derivation, we have a third type of flexion which is independent from the first and the second flexions. This causes a very serious problem, because the addition of independent parameters makes it impossible to measure the three flexions uniquely. So we have to use some constraint condition to determine uniquely flexion, but it means the measured flexion and average of the flexion depend on the selection of the constraint condition. We found that the distorted image from circular shape has only two combinations of combined flexions, called eigen flexions. It is found that the eigen flexion is independent from the constraint condition. But the average of the eigen flexion includes intrinsic noise which cannot be eliminated by averaging. We then constructed the combinations of eigen flexions called eigen flexion combinations which contain only linear terms of the intrinsic distortion. After averaging the eigen flexion combination the dependence on the intrinsic value can be eliminated. The average of the new combinations still contain the lensing shear but it can be obtained from the average of the combined shear. We confirmed using a simple numerical simulation that the average of the eigen flexion combination do not depend on the choice of the constraint and are free from the intrinsic noise.

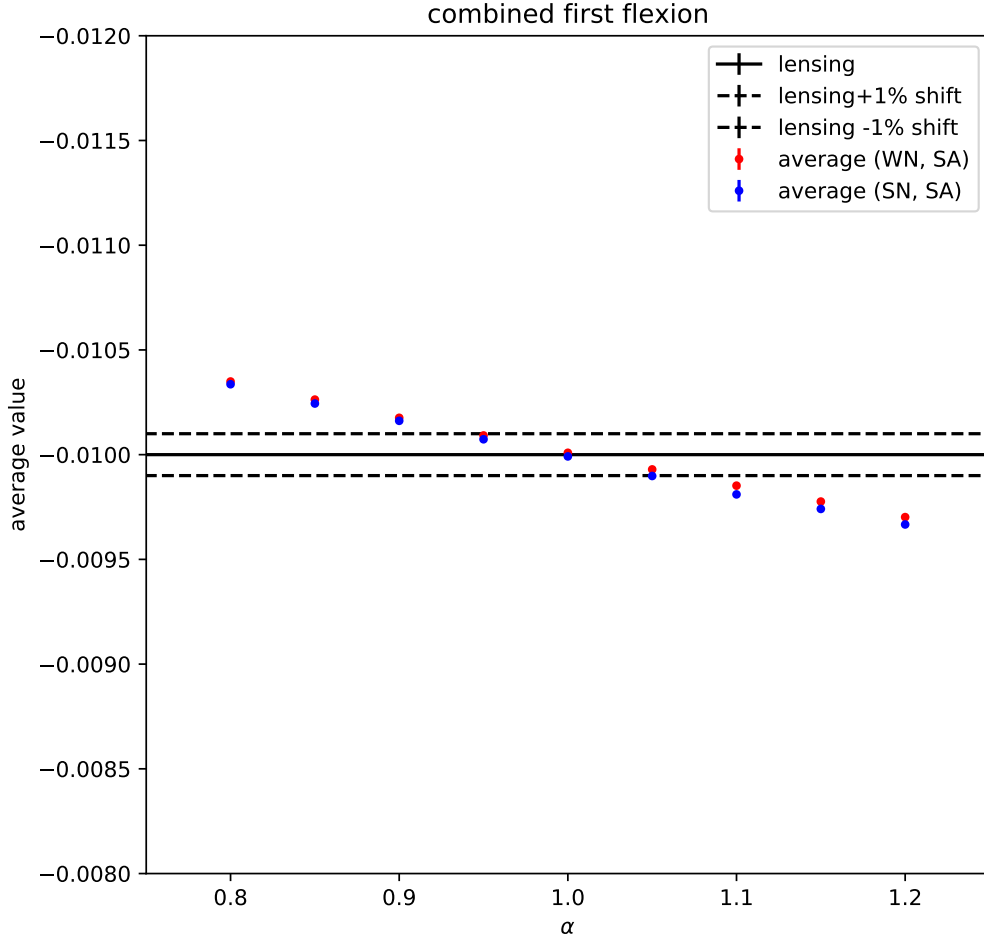


Figure 3. Same plot as figure 2 except that the red and blue points are in the case of (WN, SA) and (SN, SA) respectively.

In this way we have developed a method which can measure the lensing flexion by measuring shape of galaxy image, but there are other effects in real observation which change the shape of the image on the top of the lensed image. We need to correct them to have the lensed image before applying the method of flexion analysis developed above. One of the most important corrections is PFS correction which we will study in the next paper.

APPENDIX A: ADDITIONAL MASK FOR MOMENT MEASUREMENT

In this section we explain about the additional mask for weight function in moment measurement.

As we explained in section 2.3, a weight function which is defined as a circular function in the zero plane is used for moment measurement. The variable of the weight function is simply $|d\tilde{\beta}|$ in the zero plane, but it has nonlinear terms in the image plane and the terms make the weight function a very complex distribution. The left image of figure A1 and figure A2 are Gaussian weight functions in image plane with flexion distortions. We can see there are some peaks in the outer part from the central peak where the object is positioned. If there are other objects on the peaks, correct weak lensing information can not be obtained, so an additional mask is needed to remove the peaks. Because the peaks are in region with reversed coordinate, appropriate mask $M(\theta)$ can be obtained as

$$M(\theta) \equiv H\left(\delta\tilde{\beta}(\theta) \cdot \tilde{\beta}(\theta)\right) \quad (\text{A1})$$

$$\delta\tilde{\beta}(\theta) \equiv \frac{\partial(d\tilde{\beta})}{\partial(d\theta)}d\theta + \frac{\partial(d\tilde{\beta})}{\partial(d\theta^*)}d\theta^*, \quad (\text{A2})$$

where H is Heaviside step function. The center images of the figures are the mask regions calculated using equation A1, then the right images of the figures are masked weight. We can see the Masked weight can mask the peaks.

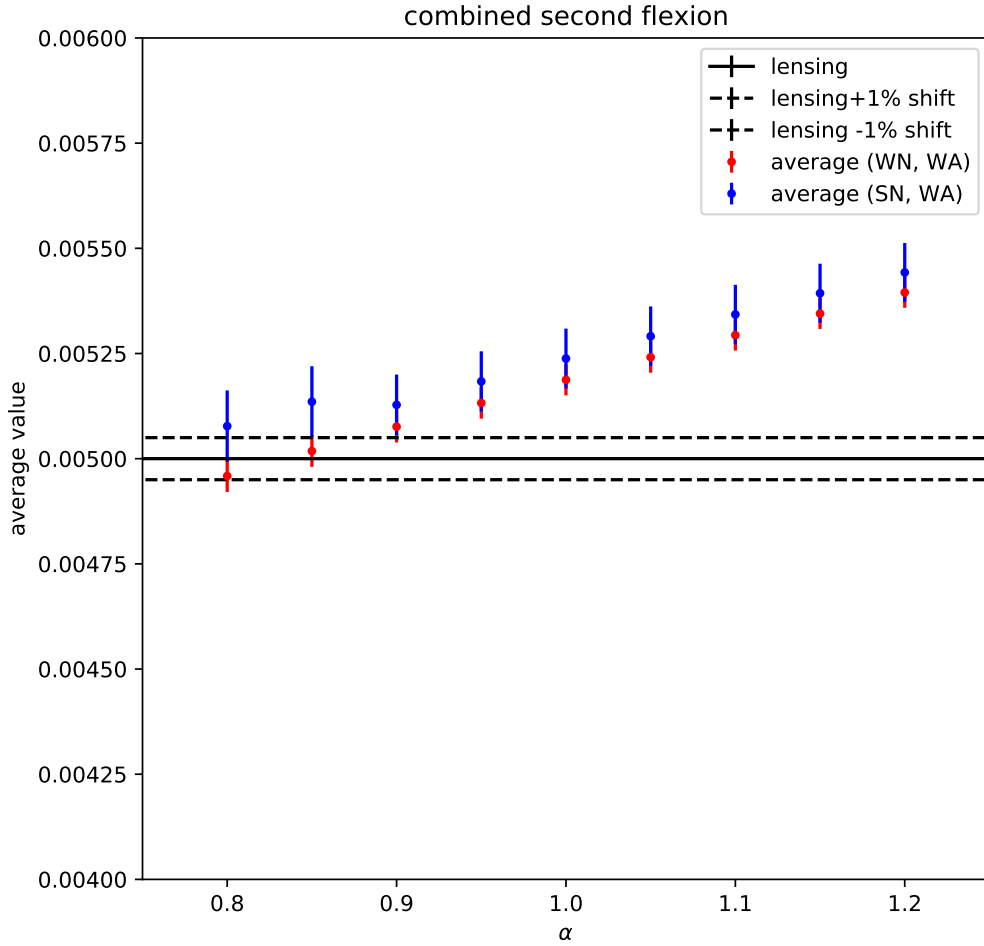


Figure 4. Same plot as figure 2 except that the red and blue points are the average value of combined second flexion in the case of (WN, WA) and (SN, WA) respectively.

ACKNOWLEDGEMENTS

This work is supported in part by a Grant-in-Aid for Science Research from JSPS (No.20K03937 to T.F).

REFERENCES

- Bacon, D. J., et al., 2006, MNRAS, 365, 414–428
 Bacon, D. J., et al., 2010, MNRAS, 409, 389–395
 Bird, J. P. and Goldberg, D. M., 2018, MNRAS, 476, 1198–1212
 Benjamin, C., Marusa, B., Rebecca, L., 2016, MNRAS, 463, 4287–4300
 Irwin, J. and Shmakova, M., 2006, ApJ, 645, 17–43, 2006
 Irwin, J., et al. 2007, ApJ, 671, 1182–1195
 Joseph, M. F., et al., 2020, MNRAS, 501, 4103–4109
 Lanusse, F., 2016, A&A, 591, A2
 Leonard, A., et al. 2009, MNRAS, 395, 1438–1448
 Levinson, R., 2013, PASP, 125, 1474–1495
 Goldberg, D. M., and Bacon, D. J., 2005, ApJ, 619, 741–748
 Goldberg, D. M., and Leonard, A., 2007, ApJ, 660, 1003–1015
 Goldberg, D. M., and Natarajan, P., 2002, ApJ, 564, 65–72
 Miller, L., et al., 2007, MNRAS, 382, 185
 Munshi, D., Valagesas P., Van Waerbeke, L. & Heavens, A., 2008, Phys. Rept. 462, 67
 Okura, Y., Umetsu, K. and Futamase, T., 2007, 660, 995–1002
 Okura, Y., Umetsu, K. and Futamase, T., 2008, 680, 1–16
 Okura, Y., Futamase, T., 2011, ApJ, 730, 9
 Okura, Y., Futamase, T., 2012, ApJ, 748, 112
 Okura, Y., Futamase, T., 2013, ApJ, 771, 37

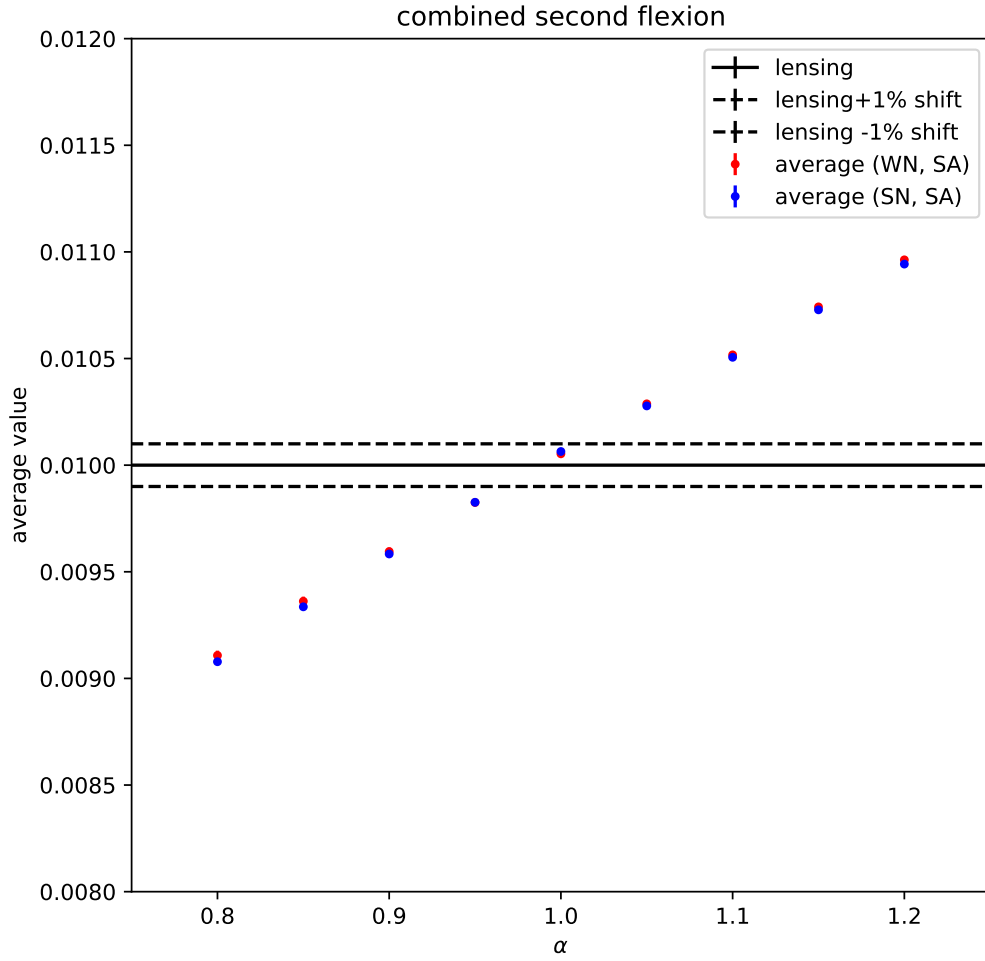


Figure 5. Same plot as figure 4 except that the red and blue points are in the case of (WN, SA) and (SN, SA) respectively.

Okura, Y., Futamase, T., 2014, ApJ, 792, 104

Okura, Y., Futamase, T., 2015, A&A, 576, 63

Okura, Y., Futamase, T., 2016, ApJ, 827, 138

Okura, Y., Futamase, T., 2018, MNRAS, 479, 4971–4983

Schneider., 2006, Part 1: Introduction to gravitational lensing and cosmology, ISBN: 3-540-30309-X

Cardone, V. F., et al., 2016, MNRAS, 462, 4028–4037

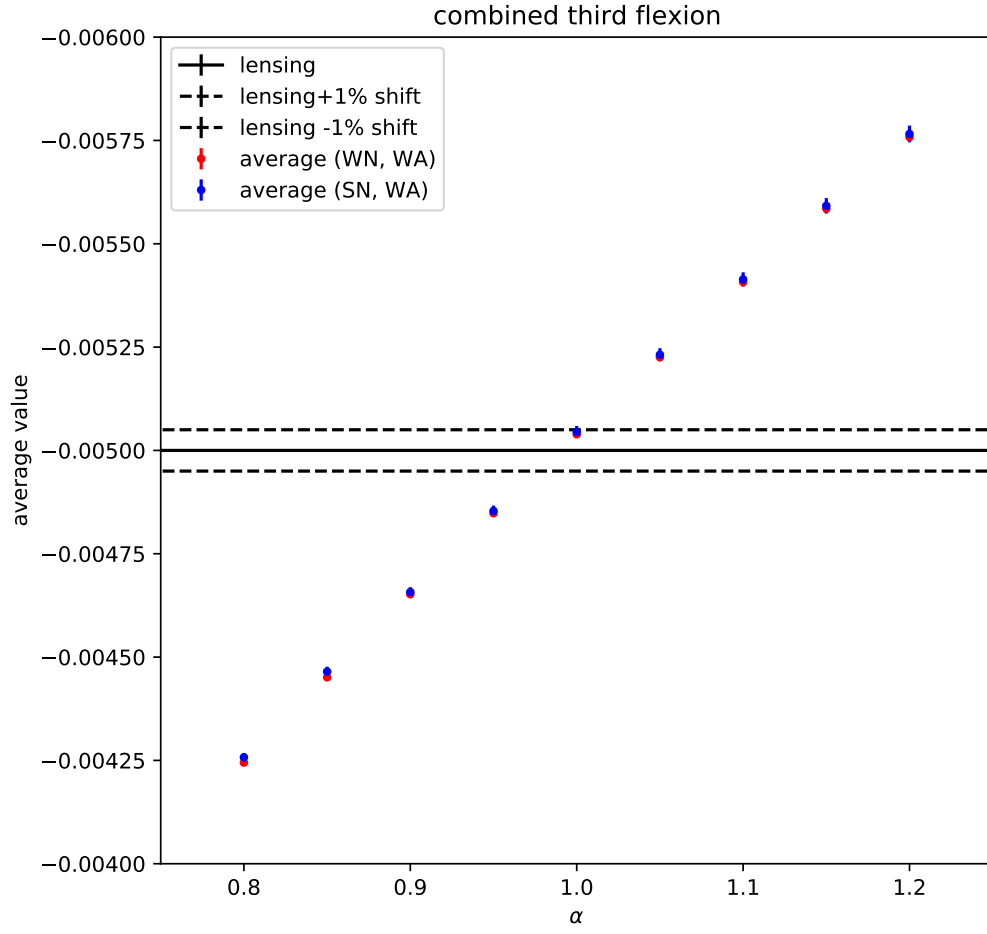


Figure 6. Same plot as figure 2 except that the red and blue points are the average value of combined third flexion in the case of (WN, WA) and (SN, WA) respectively.

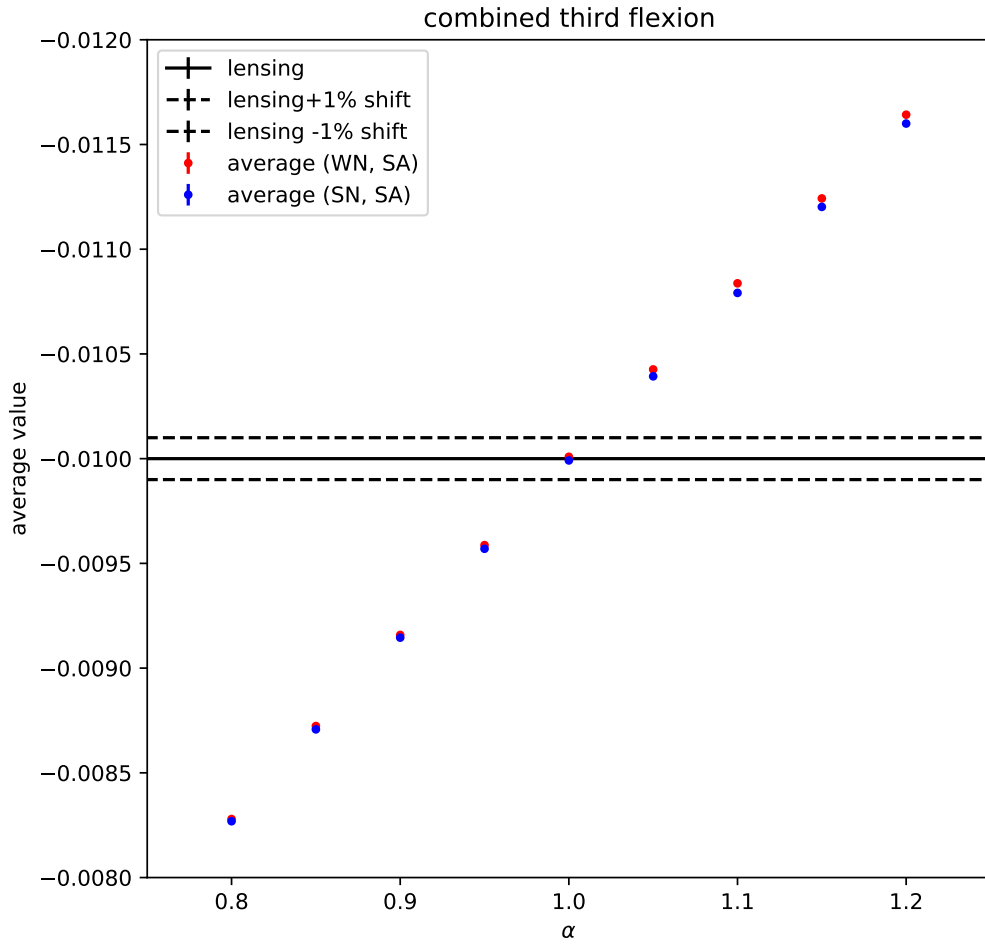


Figure 7. Same plot as figure 6 except that the red and blue points are in the case of (WN, SA) and (SN, SA) respectively.

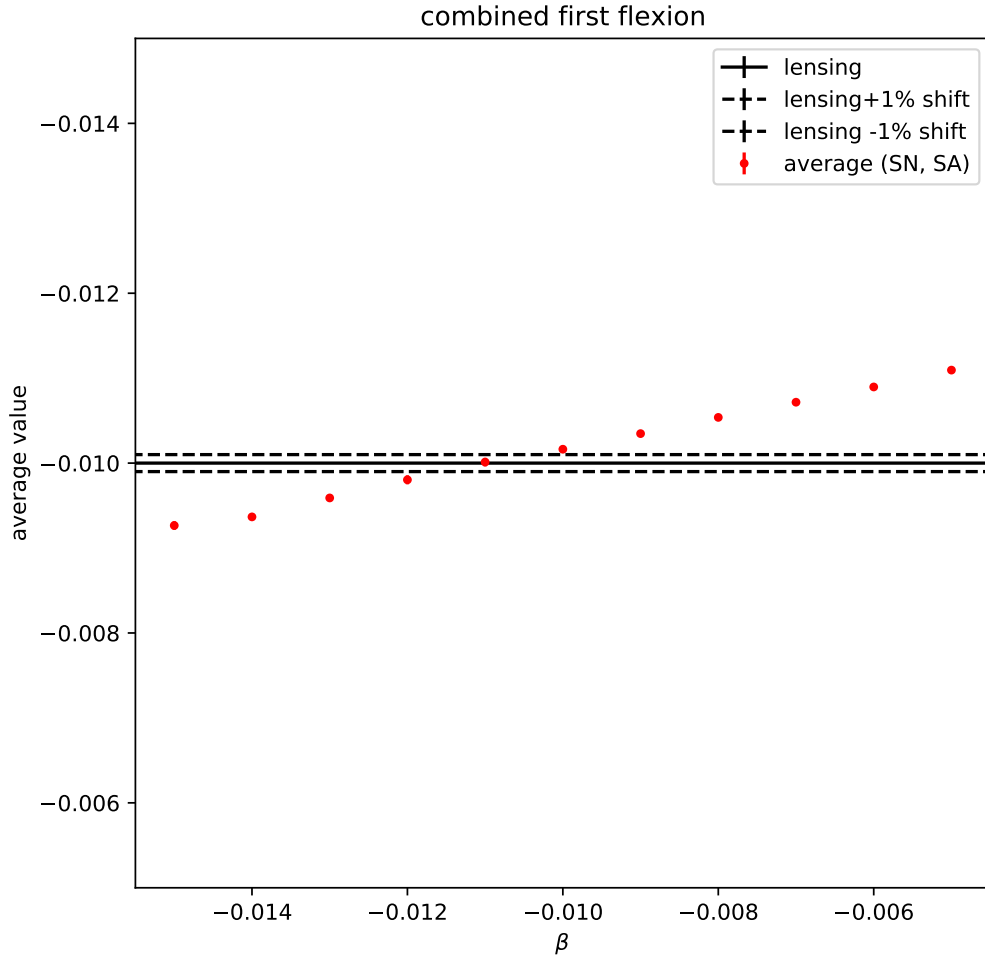


Figure 8. Same plot as figure 2 except using the second constraint condition, the horizontal axis means the constant constraint condition β and points are only (SN, SA).

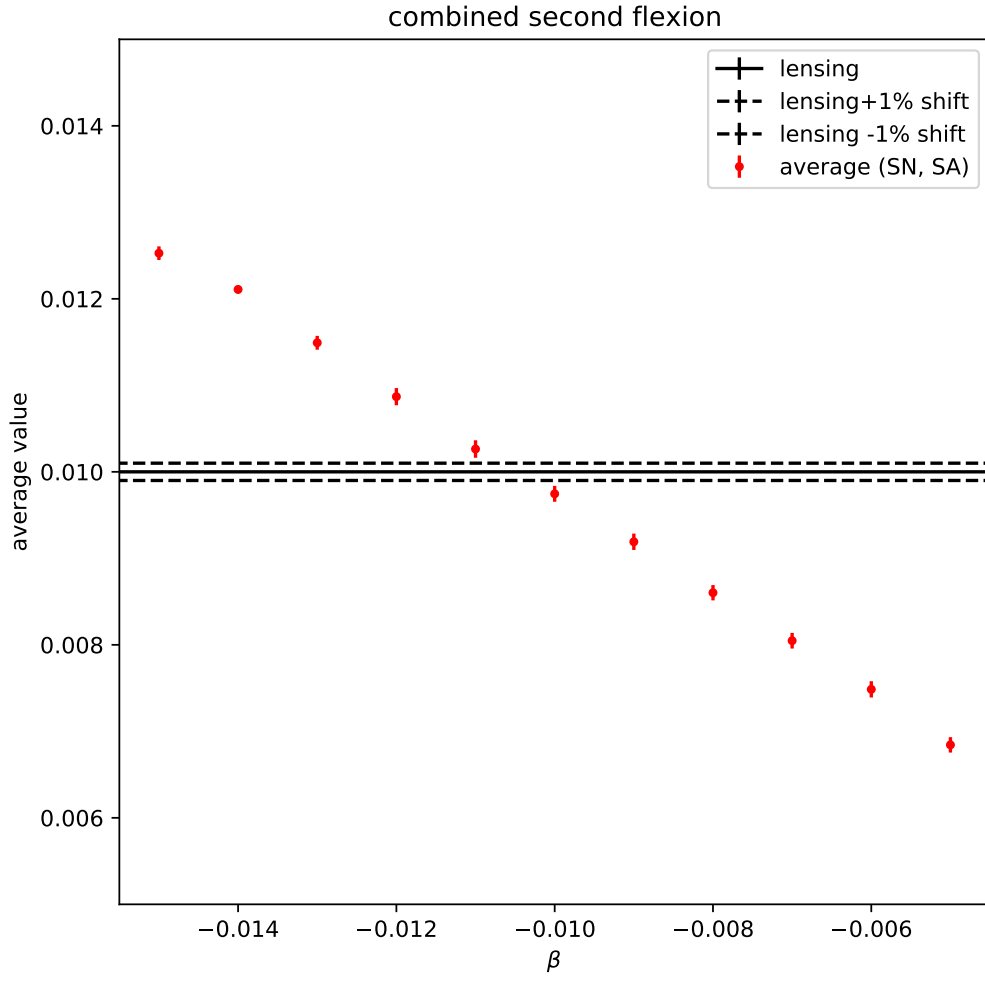


Figure 9. Same plot as figure 8 except that the red points are the average value of combined second flexion.

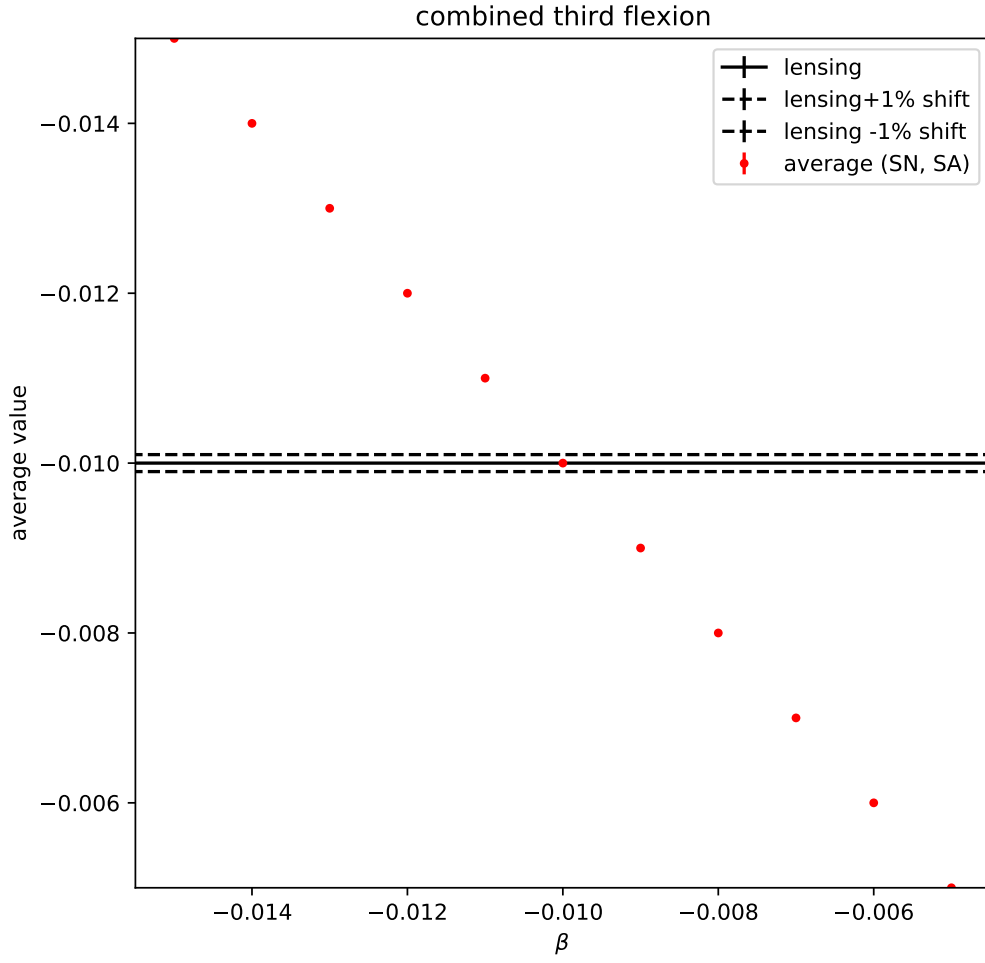


Figure 10. Same plot as figure 8 except that the red points are the average value of combined third flexion.

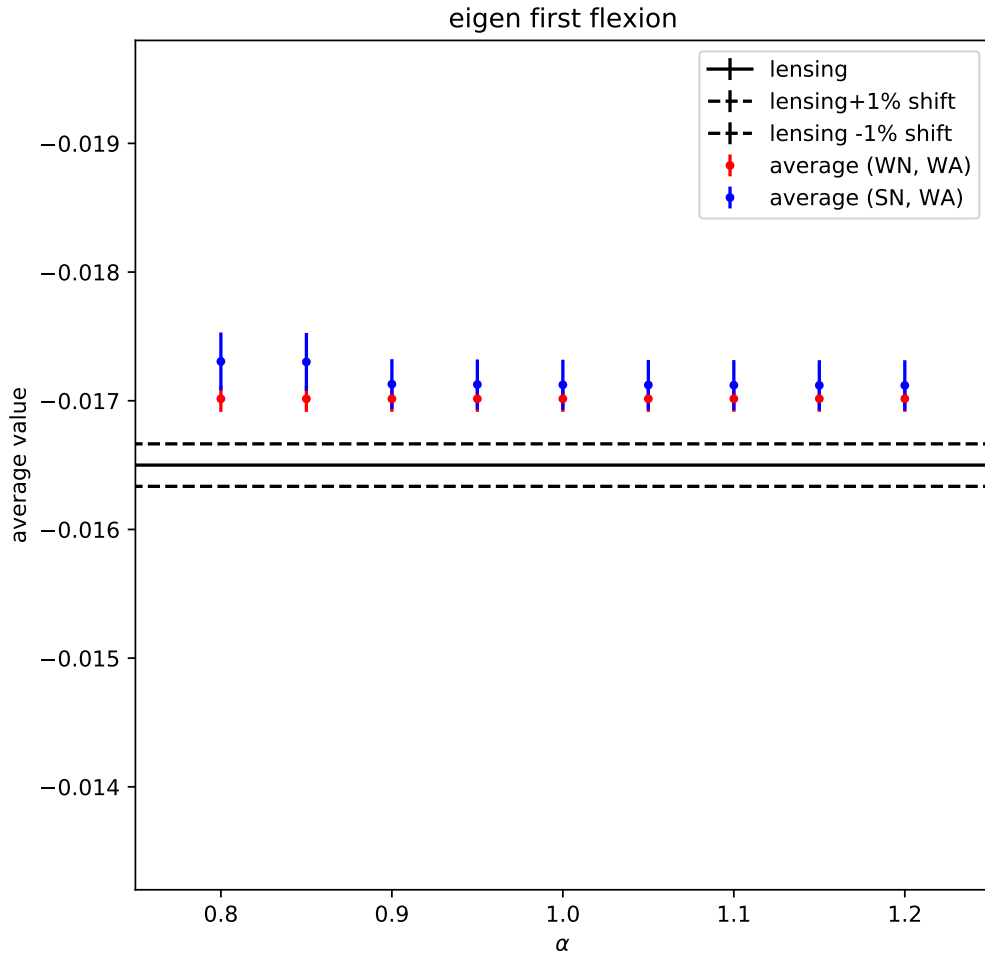


Figure 11. Same plot as figure 2 except that the red and blue points are the average value of eigen first flexion. We can see fluctuation of the average value decreases compare to the average of combined first flexion in all Cc region.

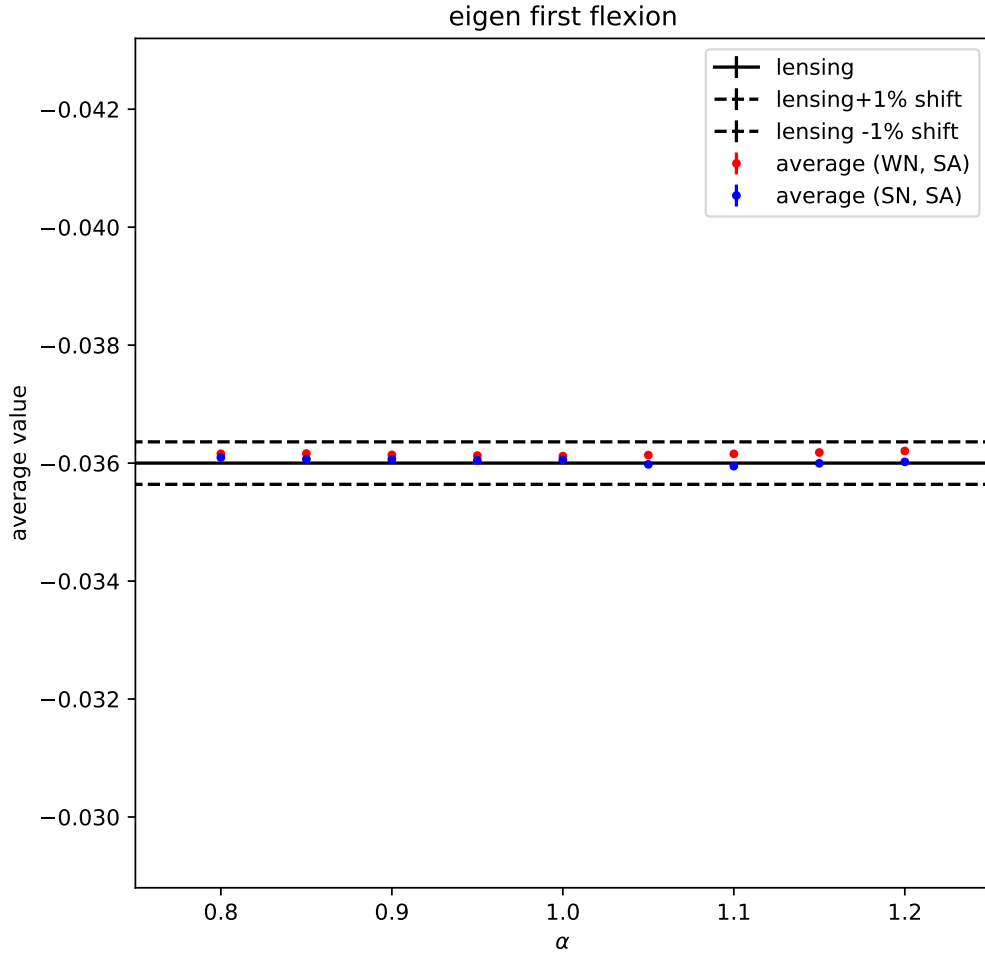


Figure 12. Same plot as figure 11 except that the red and blue points are in the case of (WN, SA) and (SN, SA) respectively.

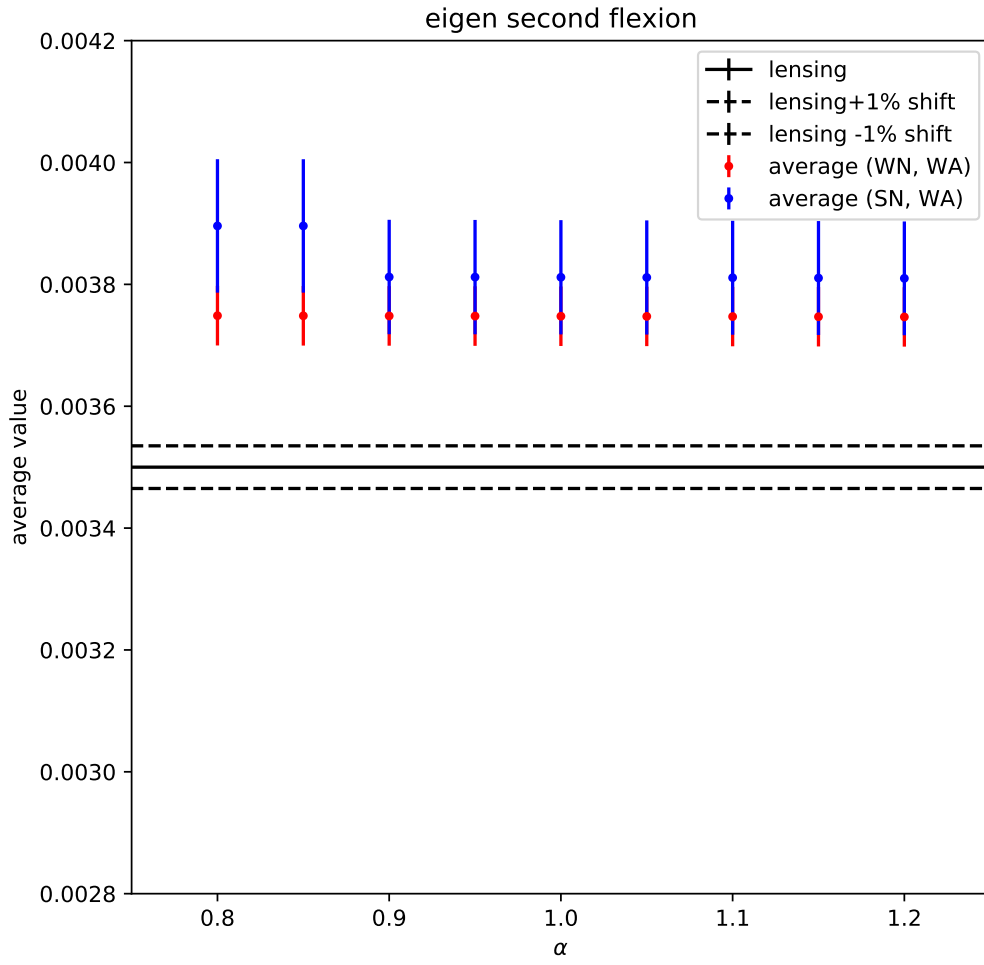


Figure 13. Same plot as figure 11 except that the red and blue points are the average value of eigen second flexion.

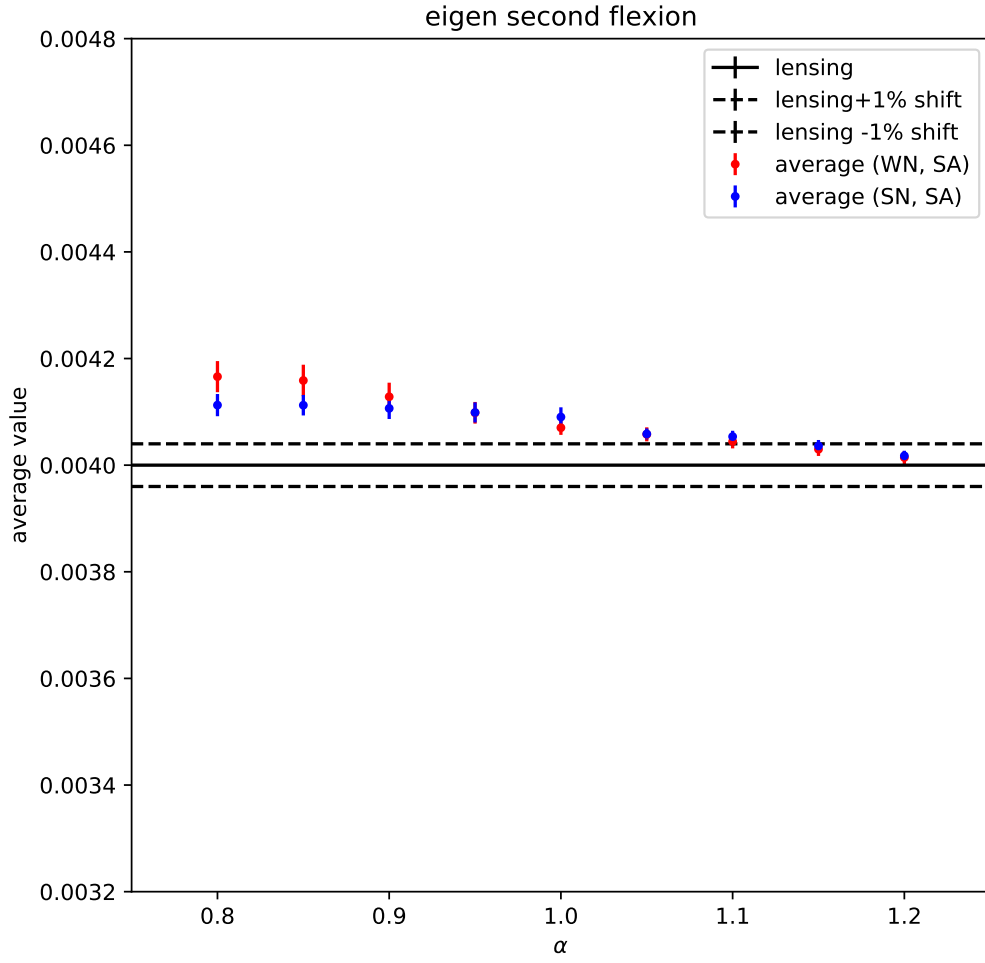


Figure 14. Same plot as figure 13 except that the red and blue points are in the case of (WN, SA) and (SN, SA) respectively.

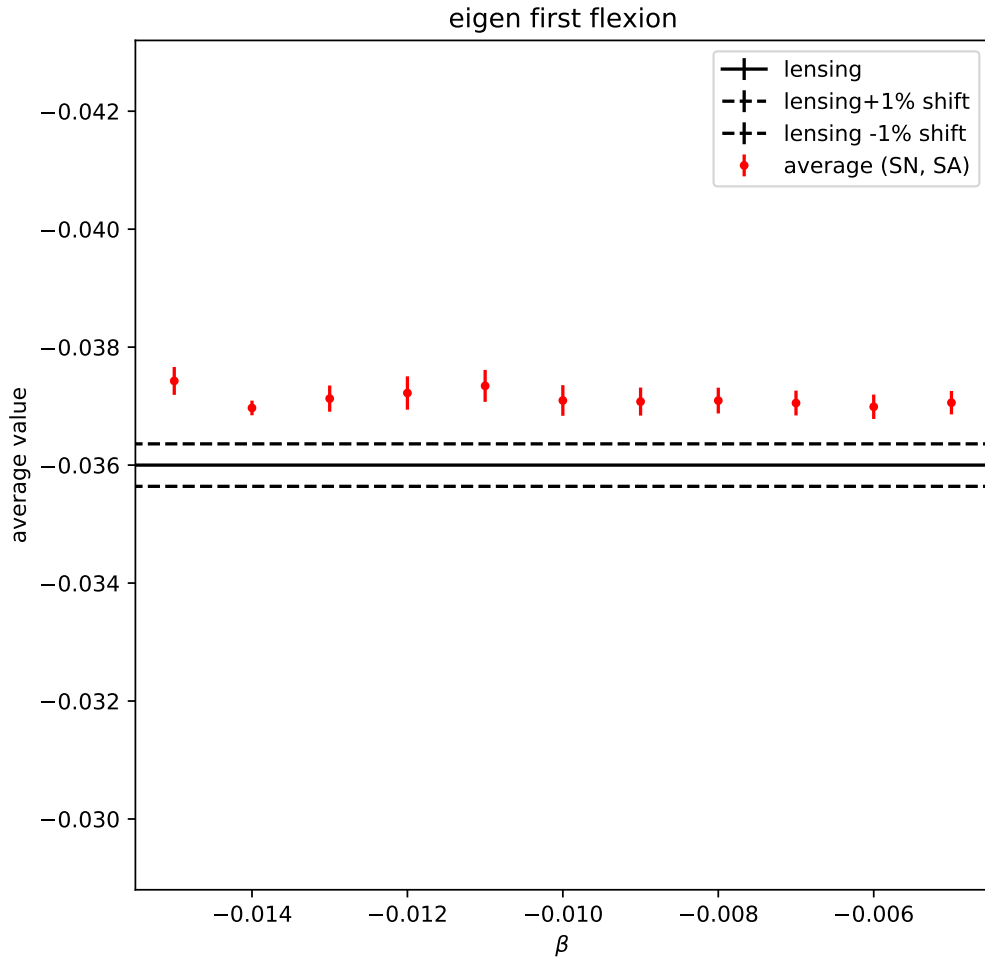


Figure 15. Same plot as figure 11 except using the second constraint condition, the horizontal axis means the constant constraint condition β and points are only (SN, SA).

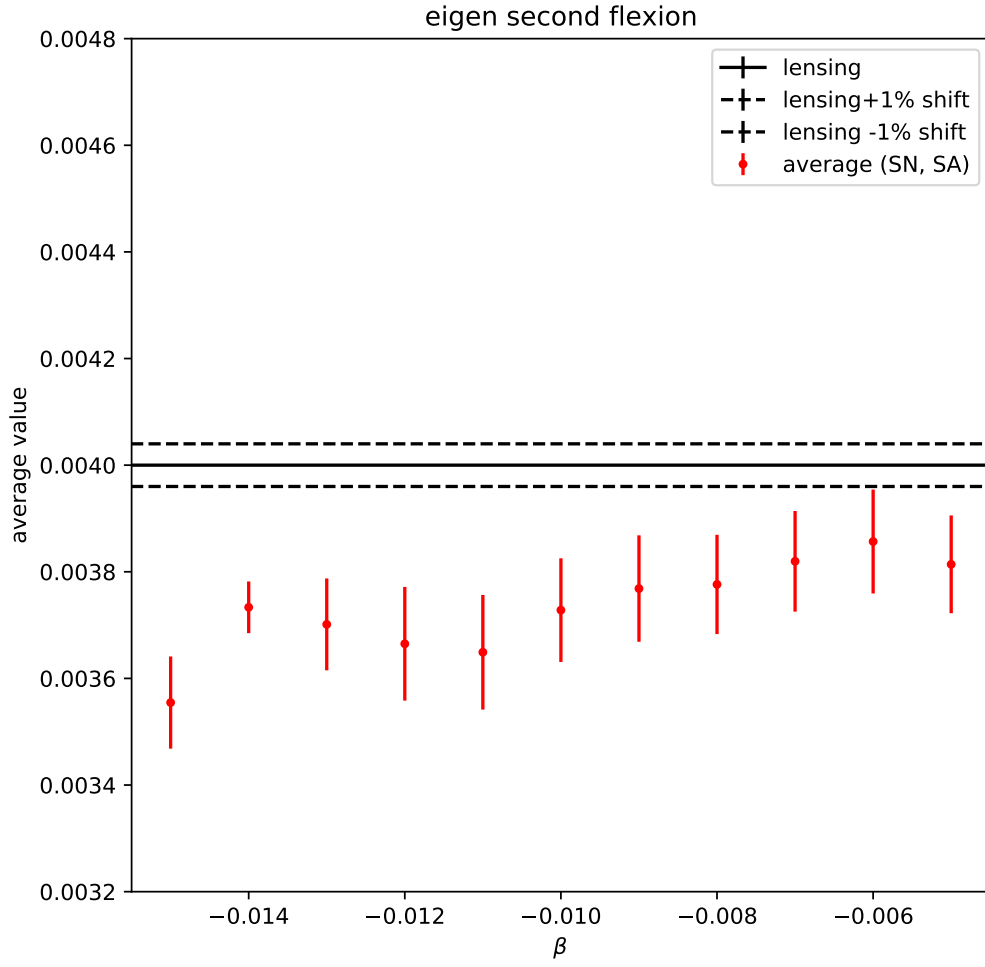


Figure 16. Same plot as figure 15 except that the red points are the average value of eigen second flexion.

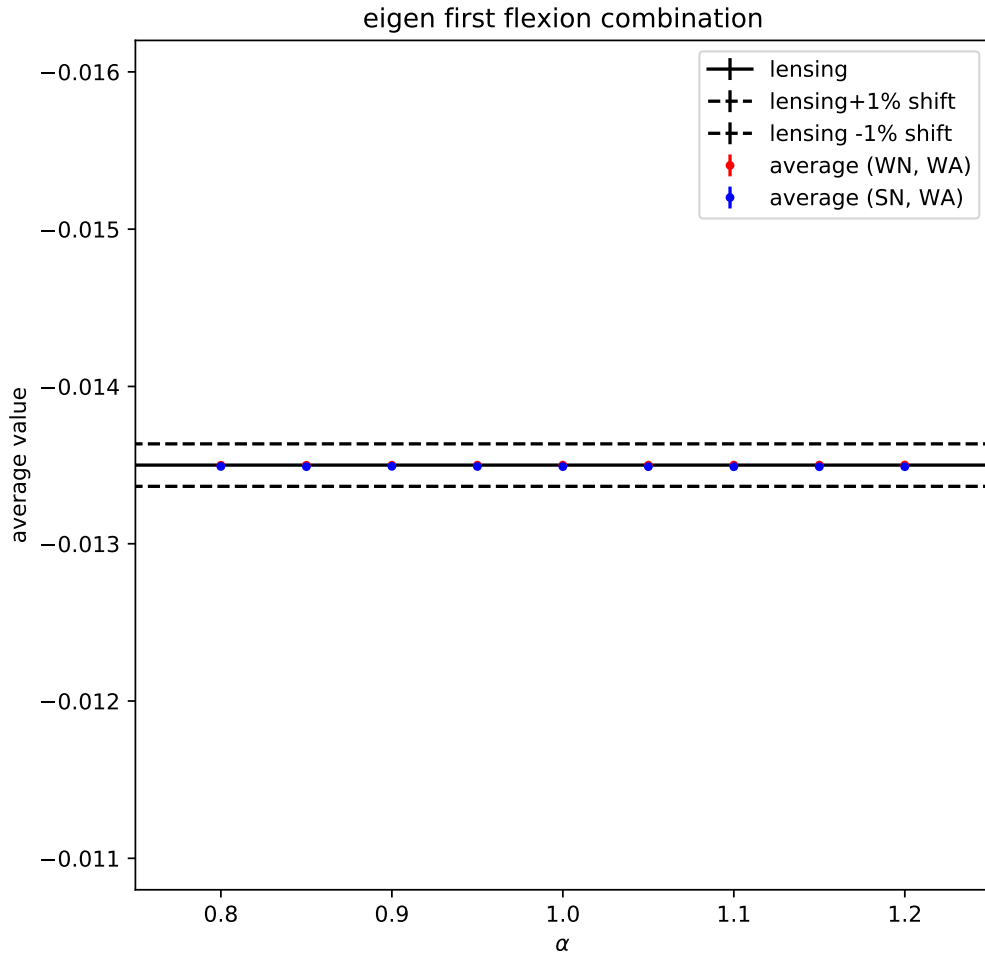


Figure 17. Same plot as figure 2 except that the red and blue points are the average value of eigen first flexion combination. We can see the average values have same value as lensing value in all Cc range.

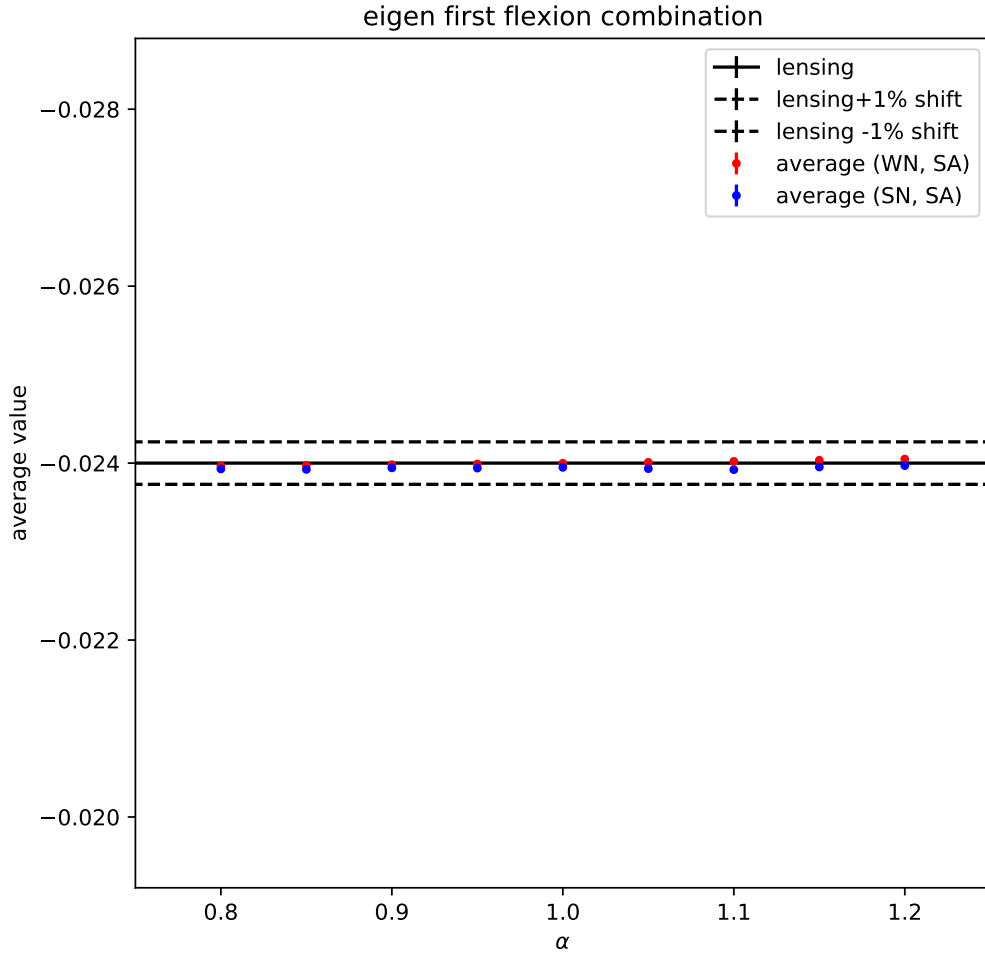


Figure 18. Same plot as figure 17 except that the red and blue points are in the case of (WN, SA) and (SN, SA) respectively.

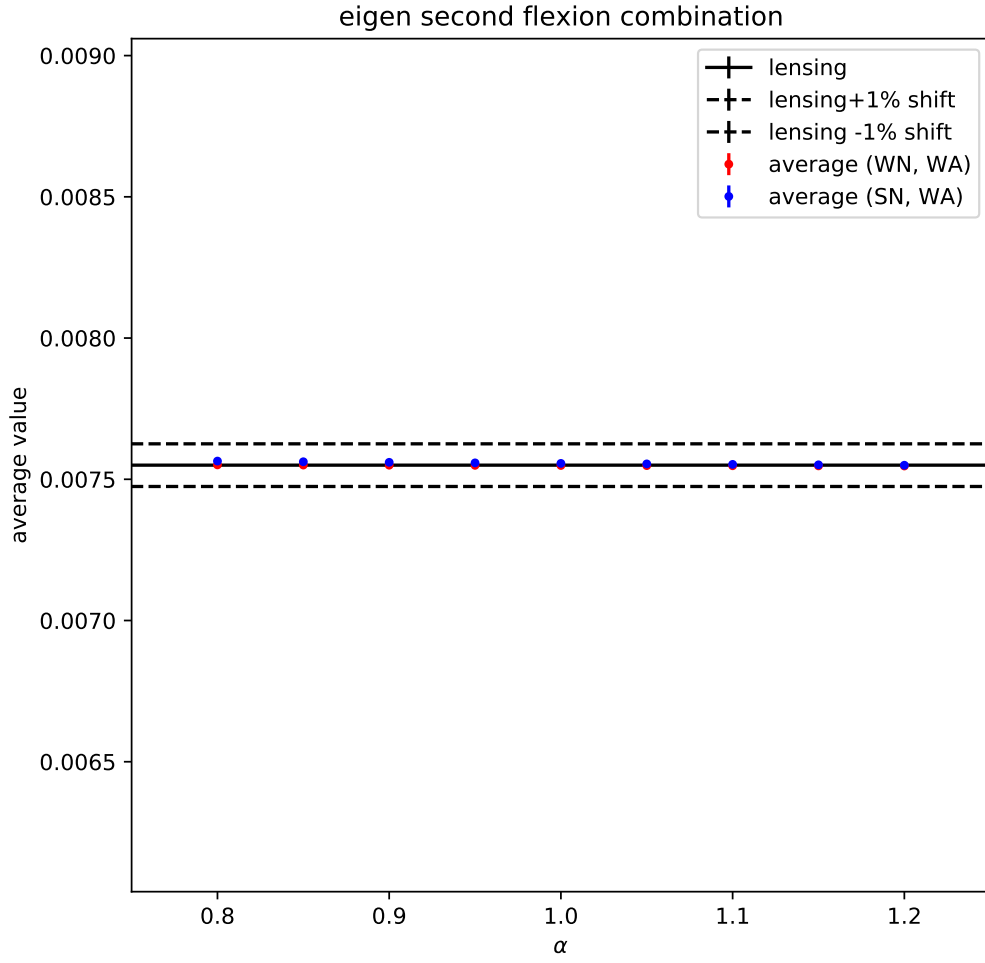


Figure 19. Same plot as figure 17 except that the red and blue points are the average value of eigen second flexion complex.

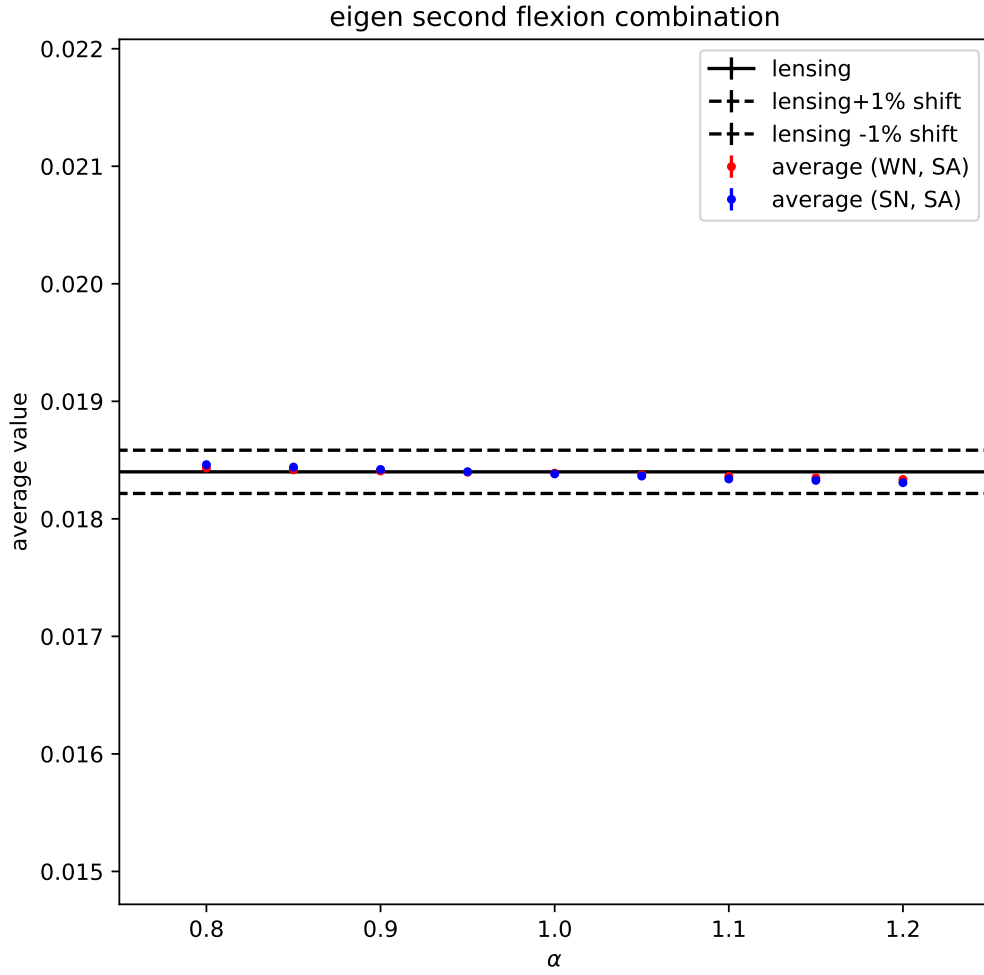


Figure 20. Same plot as figure 19 except that the red and blue points are the average value of eigen second flexion.

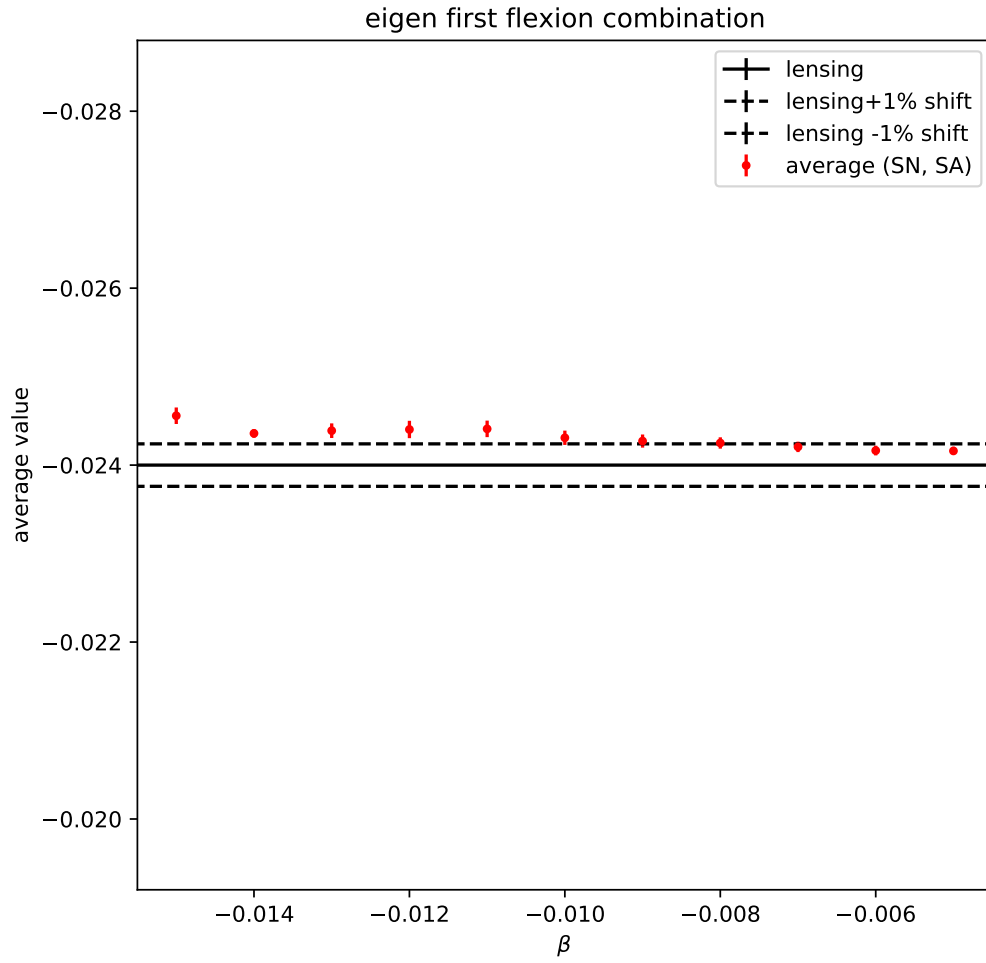


Figure 21. Same plot as figure 17 except using the second constraint condition, the horizontal axis means the constant constraint condition β and points are only (SN, SA).

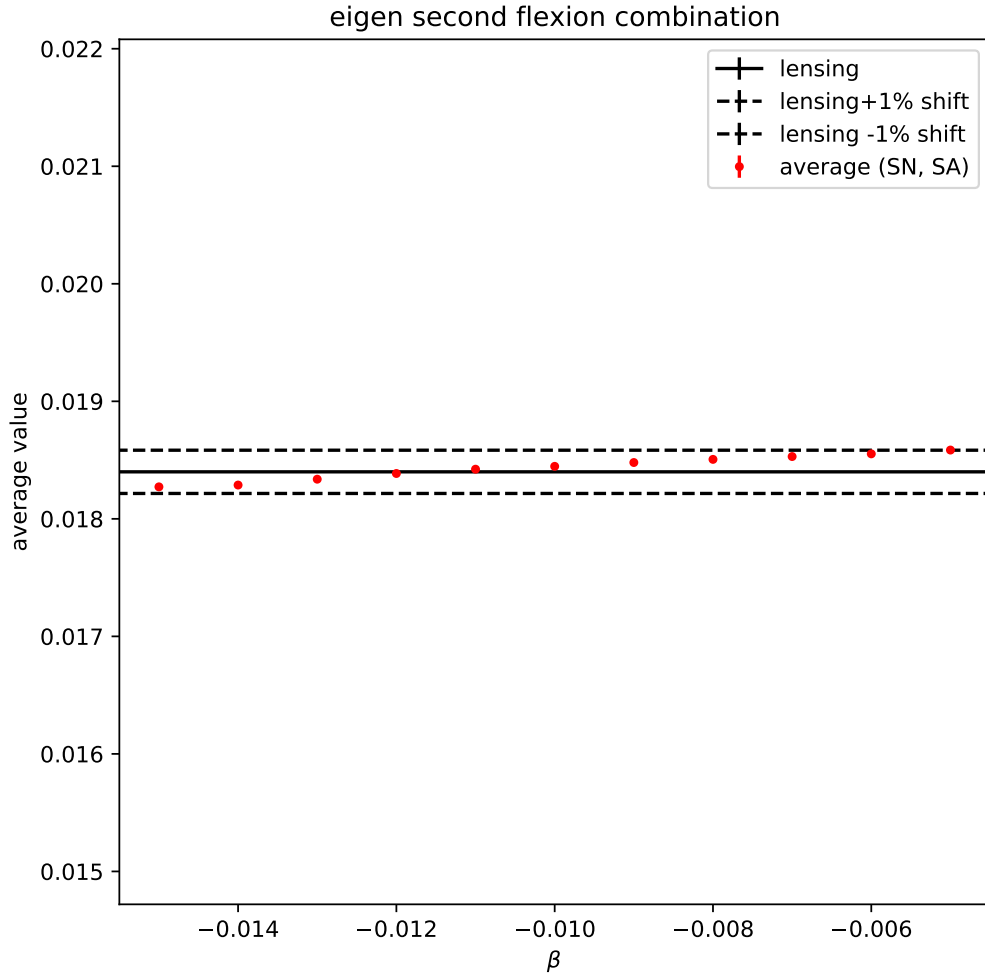


Figure 22. Same plot as figure 15 except that the red points are the average value of eigen second flexion combination.

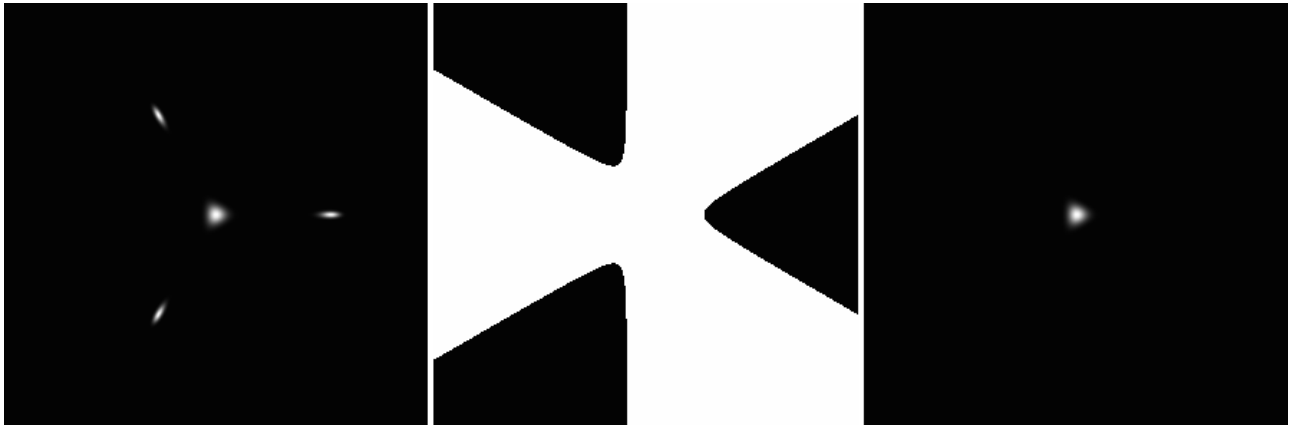


Figure A1. Weight(left), mask(center) and masked weight(right) region for image with 2nd flexion only. The black region in the center image is a masked region.

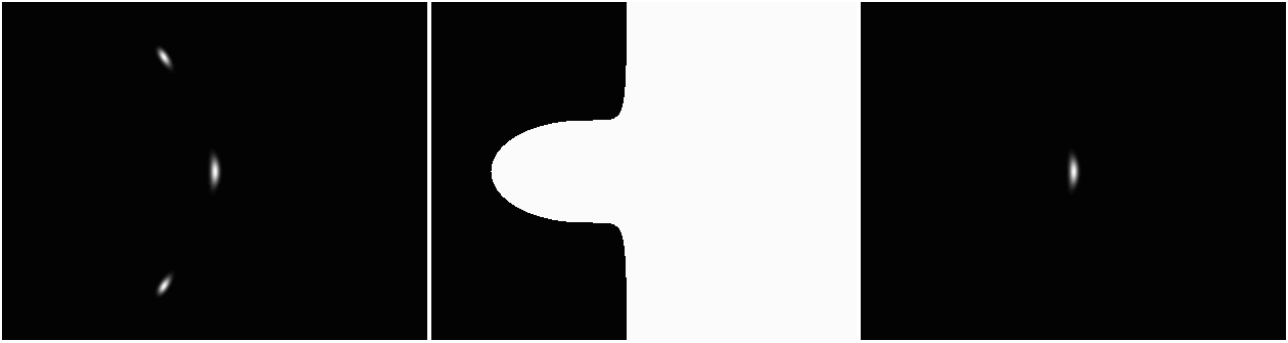


Figure A2. Same image as figure A1 except the distortion is shear and both flexions.